A semi-empirical approach for tsunami inundation: An application to the coasts of South Italy

Lorenzo Melito[1], Francesco Lalli[2], Matteo Postacchini[1]and Maurizio Brocchini[1]

[1]Department of Civil Engineering and Architecture (DICEA); Università Politecnica delle Marche, Ancona, Italy

[2]Italian Institute for Environmental Protection and Research (ISPRA); Rome, Italy

Key Points:

- A modelling chain approach for the evaluation of tsunami inundation is described and applied to the coasts of South Italy.
- The method exploits a semi-empirical extension of the classical Green's law to general bathymetries, and dedicated numerical simulations.
- The method allows for transposing computational effort from intermediate to shallow waters.

Corresponding author: Lorenzo Melito, l.melito@univpm.it

Abstract

Tsunamis in the Mediterranean Sea have been increasingly investigated in the last decades due to past destructive events. We present a novel approach for evaluating tsunami-induced coastal inundation, based on a generalization of Green's law and a chain of intermediate and small-scale numerical simulations. At the intermediate level, simulations with a linear solver are made to identify the coastal distribution of a novel parameter, namely α, condensing all nearshore wave transformations other than shoaling. α represents a proxy for coastal susceptibility to the tsunami impact. Small-scale modelling of coastal flooding performed in the southern Italy on a freely available DTM at the Esaro river estuary (Calabria) yields inundation levels that compare well with those obtained via intermediate-scale modelling, with a saving in computational time of about 41%. This demonstrates the helpfulness of α to "scale" the offshore wave input and reduce the computational effort to evaluate flooding at regional scale.

Plain Language Summary

An interest in studying the consequences of tsunamis has arisen also for the Mediterranean Sea in the last decades. In this manuscript we present a method for the evaluation of potential coastal inundation caused by the impact of tsunamis. The method exploits a chain of numerical simulations of wave propagation to move the tsunami from the source region down to the investigated coasts. The inundation estimate makes use of a simple parameter, named α, devised to encapsule all the transformation processes the tsunami undergoes in its travel from intermediate waters to the coastline. We apply the method to a portion of the Italian coast (Esaro river estuary, Calabria) with a prototype tsunami event, and we see that inundation levels achieved with faster, small-scale simulations compare well with those obtained with longer, intermediate-scale simulations. The method can be helpful as an implementation in recent tsunami warning systems developed to warn coastal communities on impending tsunami threats.

1 Introduction

The Mediterranean Sea has been subjected since millennia to the action of tsunamis (Ambraseys & Synolakis, 2010; Maramai et al., 2014), yet research interest has seen a boost only recently, in the aftermath of catastrophic events like the Indian Ocean, 2004 (Lay et al., 2005) and Tohoku, 2011 (Fujii et al., 2011; Mori et al., 2011) tsunamis. The high

level of seismic activity characterizing the Mediterranean basin and the ubiquity and richness of coastal communities thriving along its coasts spark the need for studies devoted to characterize tsunami propagation within the Mediterranean Sea and, ultimately, their impact on coastal vulnerability. However, recent applications of vulnerability and risk assessments usually take into account important hydrodynamic variables, e.g. sea-level rise, wave height, tide range (Bonaldo et al., 2019; Da Lio & Tosi, 2019; Mattei et al., 2019; Hzami et al., 2021), but disregard the potential contribution of tsunamis (Chaib et al., 2020; Anfuso et al., 2021).

The potential coastal risk induced by a tsunami wave is function of its energy, which depends on the processes the tsunami experiences while it approaches the coast, e.g. shoaling, refraction, diffraction. Since tsunami waves of similar intensity may present significantly different features when propagating over different bathymetries (Satake, 1988; Madsen et al., 2008), tsunami-seabed interaction is fundamental for a proper modelling of long wave evolution and impact. This consideration has sparked our search for an unified modelling approach to effectively consider bathymetry-related processes in tsunami modelling, while conserving general applicability, scientific soundness and ease of execution.

This work presents a methodology for the modelling and prediction of tsunami-induced coastal inundation. At the core of this methodology is a semi-analytical approach, which combines theoretical grounds and nearshore hydrodynamic modelling to encase the effects of all tsunami transformations into a single, easily understandable parameter. To scale the inputs of the procedure from basin-level down to local coasts, a modelling chain concept is applied, as already done in several coastal applications with good results (Federico et al., 2017; Gaeta et al., 2018; Postacchini et al., 2019; Postacchini & Ludeno, 2019). A practical example of the methodology is here applied to a coastal area of the Calabria region, exposed to tsunami waves approaching in an almost perpendicular direction.

The modelling chain and the proposed semi-analytical approach are described in Section 2. Results are given in Section 3 and discussed in Section 4, along with concluding remarks.

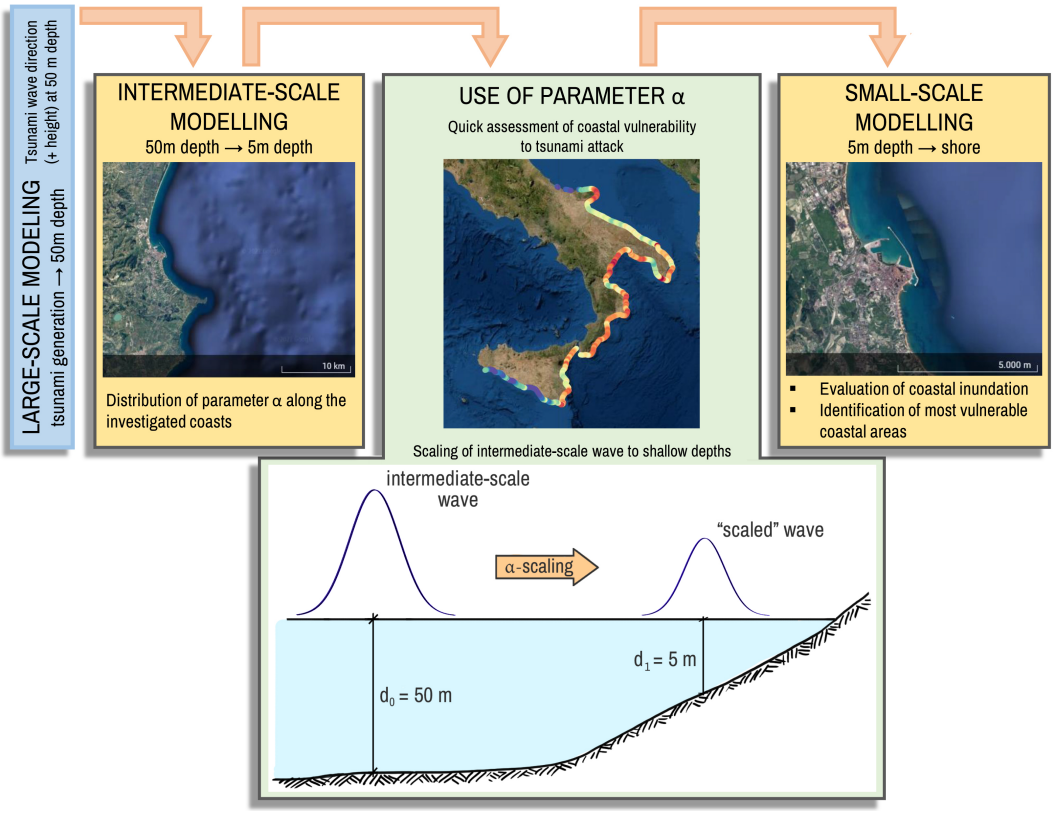

Figure 1. Conceptual scheme of the modelling chain.

2 Methods

2.1 Modelling chain

A conceptual map of the modelling chain is given in Figure 1. The first step of the procedure is tackled with a realistic approach: a tsunami wave is generated at a hypothetical earthquake epicenter located in the Hellenic arc, notoriously the most seismically active region of the Mediterranean Sea (Figure 2). The initial surface displacement then propagates across the Mediterranean basin in a *large-scale modelling*, to infer realistic tsunami front directions at intermediate depths in front of the coasts of interest (an extraction depth of 50 m has been chosen in this application).

In the second step, a separate set of numerical simulations is run (*intermediate-scale modelling*), in which tsunami-like waves are propagated from intermediate waters to the nearshore region in front of the southern Italian coasts (Apulia, Basilicata, Calabria, Sicily; orange outline in Figure 2), which are the most prone to inundation from tsunami waves generated in the Hellenic arc (Maramai et al., 2021). The purpose of intermediate-scale modelling is to gather an along-coast distribution of a parameter (α) which has been devised to serve as a proxy for the several processes (e.g., shoaling, refraction, diffraction) that the modelled tsunami, given a propagating direction derived from the previous large-scale modelling, will undergo during its propagation from intermediate to shallow waters.

After the parameter distribution is obtained, values of α are used in the third step as a "scaling factor" to transport the properties of the tsunami wave from intermediate depths (i.e., the wave shape used as input for the intermediate-scale modelling) up to shallow waters, as described in Section 2.4. The so-scaled wave, which is now assumed to have undergone all the transformation processes represented by α, is used as an initial condition for a *small-scale modelling*, to finally get an estimate of coastal inundation.

2.2 The analytical solution: Green's law generalization

Lalli et al. (Lalli et al., 2019) have proposed a semi-analytical approach to characterize the transformation process of tsunami-like long waves over general bathymetries: the approach involves a generalization of Green's law (Dean & Dalrymple, 1991) with

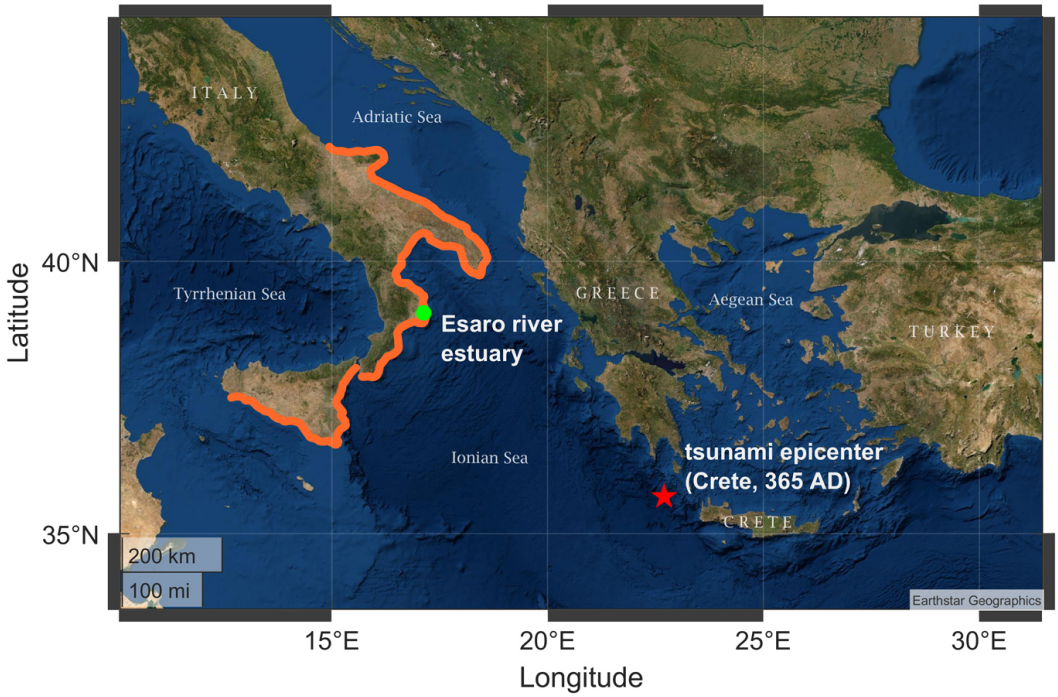

Figure 2. Map of central Mediterranean Sea. The southern Italian coast chosen for the evaluation of α (orange outline), the Esaro river estuary (green circle) and the epicentre of the prototype tsunami event (red star) are shown.

a generalizing parameter α:

$$H_1 = \alpha\, H_0 \left(\frac{d_0}{d_1}\right)^{1/4} \tag{1}$$

where H_0 and d_0 are the wave height and depth at an offshore location (or in deep water), and H_1 and d_1 are the respective values at a location closer to the shore. α is to be evaluated empirically with the use of suitable numerical simulations of long wave propagation over the complex bathymetry of interest. α is calculated as

$$\alpha = \sqrt{\frac{\tilde{\Phi}_1}{\tilde{\Phi}_0}} \tag{2}$$

where $\tilde{\Phi}_1$ is the time-cumulative energy flux of the long wave evaluated at any given depth d_1, and $\tilde{\Phi}_0$ is the flux at an offshore location d_0. α can be considered as a proxy of how much the tsunami energy flux changes as it travels from the deep sea to shallow waters, by virtue of processes other than pure shoaling. The linear approximation of the specific energy flux is

$$\Phi = g d \eta\, |V| \tag{3}$$

where η is the surface elevation, d is the undisturbed water depth, and V is the depth-averaged fluid velocity.

In a sense, α is similar in concept to the classical refraction coefficient adopted to model the change in wave height due to refraction. However, it assumes a much broader meaning when evaluated by numerical modelling, as it also encompasses every contribution to long waves transformation other than shoaling, e.g. reflection, diffraction and other interactions with natural obstacles and artificial structures.

2.3 The shallow-water model

The α parameter of Equation (2) is numerically evaluated with flux data from numerical simulations of long wave propagation at an intermediate-scale. In the present application, simulations are performed using the model SASHA (Staggered ANPA SHallow wAter; Lalli et al. (2001, 2010)), which solves the shallow water equations with a finite difference scheme deployed on a staggered Cartesian grid. Such equations represent the conservation of mass and momentum:

$$\frac{\partial \eta}{\partial t} + \frac{\partial U}{\partial x} + \frac{\partial V}{\partial y} = 0, \tag{4}$$

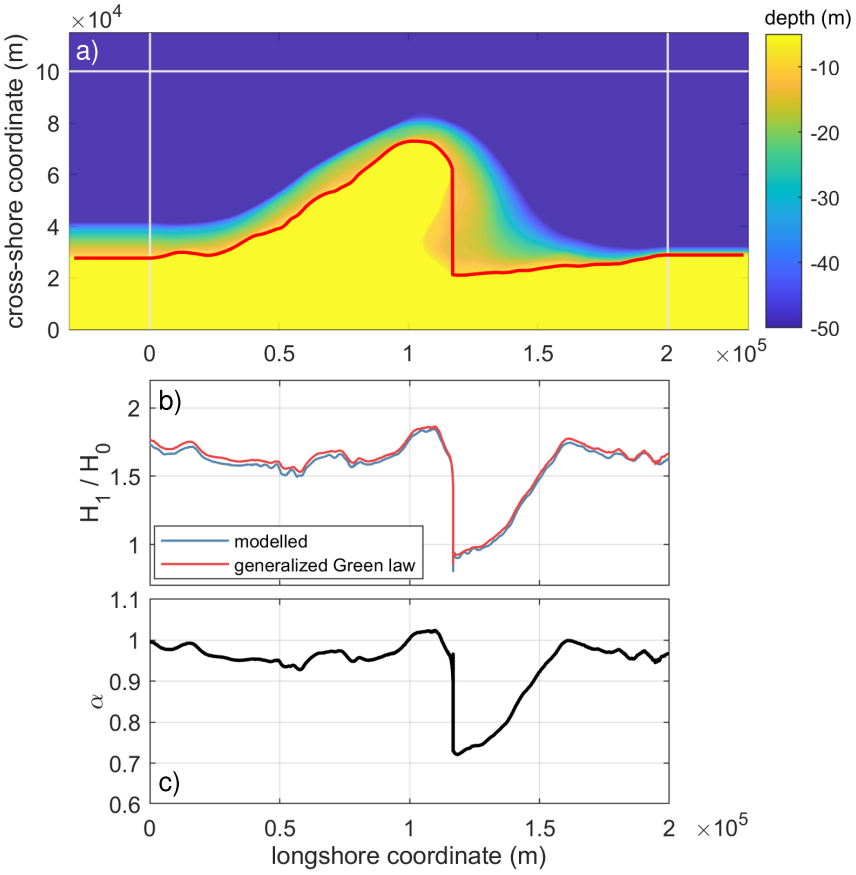

Figure 3. Configuration and output of a typical intermediate-scale simulation with SASHA; **a)** numerical domain. The 5-m isobath (red line) and the limits of the sponge layers (grey lines) are shown; **b)** H_1/H_0 at the 5 m isobath, modelled by SASHA (blue line) and evaluated with Equation (1) (red line); **c)** distribution of modelled α along the 5-m isobath.

$$\frac{\partial U}{\partial t} + \frac{\partial (U^2/h)}{\partial x} + \frac{\partial (UV/h)}{\partial y} = \\ = -gh\frac{\partial \eta}{\partial x} + 2\,\frac{\partial}{\partial x}\left(\mu h \frac{\partial u}{\partial x}\right) + \frac{\partial}{\partial y}\left[\mu h \left(\frac{\partial v}{\partial x} + \frac{\partial u}{\partial y}\right)\right] - F_u U, \tag{5}$$

$$\frac{\partial V}{\partial t} + \frac{\partial (UV/h)}{\partial x} + \frac{\partial (V^2/h)}{\partial y} = \\ = -gh\frac{\partial \eta}{\partial y} + 2\,\frac{\partial}{\partial y}\left(\mu h \frac{\partial v}{\partial y}\right) + \frac{\partial}{\partial x}\left[\mu h \left(\frac{\partial v}{\partial x} + \frac{\partial u}{\partial y}\right)\right] - F_v V. \tag{6}$$

The term μ, assumed constant, includes both molecular and eddy viscosity components; F_u and F_v represent friction factors. u and v are depth-averaged horizontal velocities in the x and y directions; h is the total water depth and $U = hu$, $V = hv$. Finally, the total local water depth is approximated with the undisturbed depth ($h \approx d$), so that $U \approx hu$ and $V \approx hv$. Further details can be found in Lalli et al. (2001, 2010, 2019).

Intermediate-scale simulations in SASHA have been performed for each subdomain into which the southern Italy coastlines has been divided into (Figure 5). An absorbing layer, whose length is equal to half the length of the input prototype wave, has been placed at the landward edge of the modelled region to dissipate the residual wave energy once the long wave has trespassed the 5 m depth isobath. Sponge layers have also been placed at the seaward and lateral sides of the domain to absorb spurious reflected waves.

On the basis of preliminary tests, solitary waves have been set up at the offshore boundary of each domain and then propagated between 50-m and 5-m depths, bearing in mind that SASHA is a linear model and its results are independent of the wave height imposed at the offshore boundary (Lalli et al., 2019). The nearshore cumulative energy flux $\tilde{\Phi}_1$ is estimated with Equation (3) after the whole wave has traveled through the 5 m isobath, and finally used to evaluate α by means of Equation (2).

An example of the setting and output of a typical intermediate-scale simulation with SASHA is given in Figure 3 for the Gargano headland (Apulia). Figure 3a shows the bathymetry over which the input wave propagates and the 5-m isobath at which the energy flux is calculated (red line). Figure 3b shows the ratio H_1/H_0 as directly modelled by SASHA (blue line) and as evaluated semi-analytically with the generalized Green's law (red line).

A good correspondence of the two curves gives confidence in the method. Values of α along the 5-m isobath are given in Figure 3c.

2.4 Methodology for the assessment of flooding

The distribution of α along any given coast is finally employed to "scale" the tsunami wave properties, i.e. to evaluate its height and length in shallow waters (depth $d_1 = 5$ m), once the height at intermediate depth ($d_0 = 50$ m) is known. A conceptual scheme of the scaling process to move intermediate-scale wave input towards shallow depths is given in the bottom panel of Figure 1.

The shallow-water wave height H_1 is first calculated by Equation (1), with α taken as the mean value $\overline{\alpha}$ along the coastal stretch being investigated:

$$H_1 = \overline{\alpha}\, H_0 \left(\frac{d_0}{d_1}\right)^{1/4}. \tag{7}$$

Under the commonly assumed hypothesis that the wave period is conserved between d_0 and d_1, the shallow water wave length L_1 is then calculated by the definition of the solitary wavenumber provided in Madsen et al. (2008):

$$L_1 = \frac{2\pi}{k_1} = 4\pi d_0 \sqrt{\frac{d_1}{3H_0}} \tag{8}$$

where k_1 is the wavenumber of the solitary wave in shallow waters. L_1 is therefore taken as the tsunami wavelength at depth d_1. A solitary wave characterized by wave height H_1 and length L_1 has been finally applied as initial condition at depth d_1, to be used for the shallow-water simulation for the evaluation of shoreline motion and coastal inundation.

3 Results

3.1 Large-scale modelling: tsunami propagation in the Mediterranean Sea

One of the most catastrophic seismic events in the history of the Mediterranean Sea occurred in 365 A.D. (Stiros, 2001), with epicenter to the West of Crete island, in the Hellenic arc (the red star in Figure 2). A simple numerical recreation of this tsunami is considered in our application, to evaluate the global impact of a typical tsunami on southern Italian coasts and estimate the main approach direction of the long wave front. Although the main focus of our work is to define a semi-empirical procedure based on

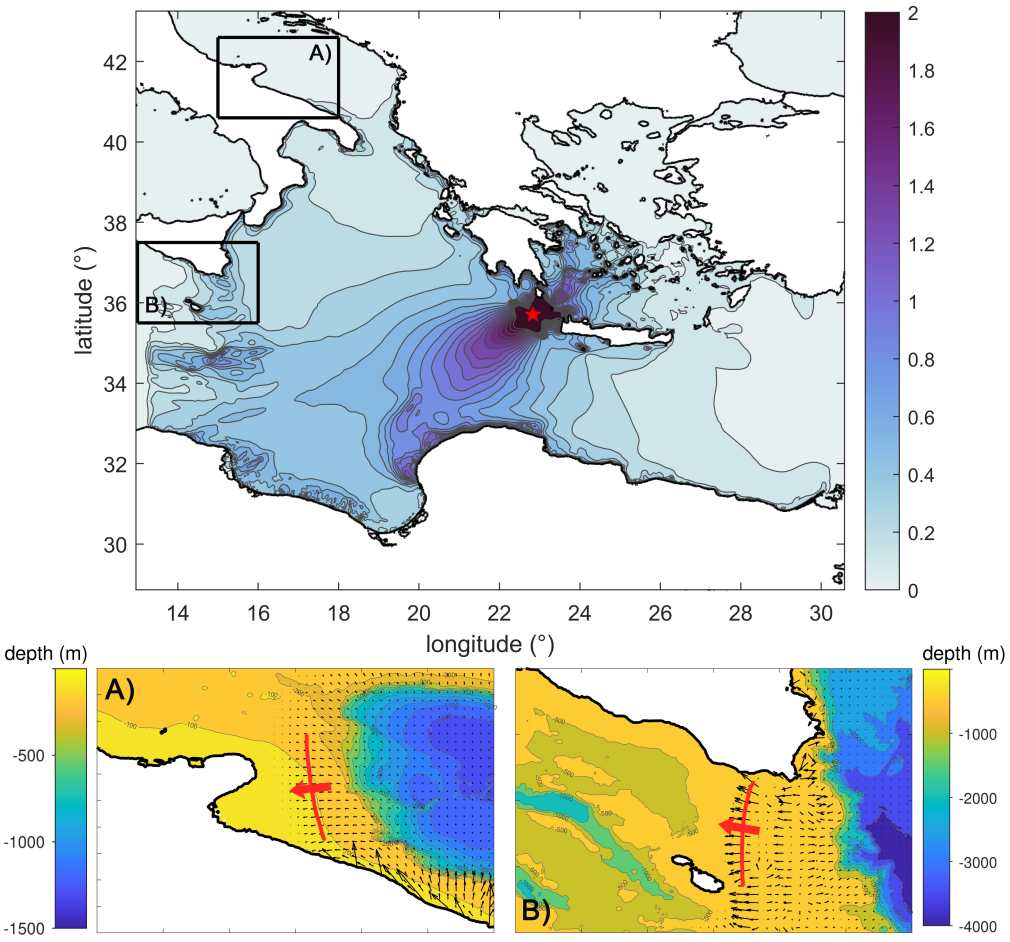

Figure 4. Map of the maximum water level modelled by FUNWAVE-TVD for a prototype tsunami originated from the Hellenic arc, west of Crete Island (red star). The modelled approach directions of the tsunami wave front (red lines and arrows) for Apulia and southern Sicily are highlighted in panels **A)** and **B)**. Black ectors represent the modelled tsunami wave velocity fields.

a linear solver and illustrate its application, a preliminary modelling with the renowned nonlinear solver FUNWAVE-TVD (Shi et al., 2012) is made on a basin level.

A Gaussian hump has been used to model a prototype tsunami originating in the west Hellenic Arc. The hump has a maximum height of 5 m, while its major axis has an orientation of 45°N to follow the direction of the local underwater fault. The numerical grid covering the central part of the Mediterranean Sea has been built using bathymetric data available at the online platform GEBCO (Weatherall et al., 2015).

Figure 4 illustrates the maximum modelled water elevation in the central Mediterranean Sea. The output of such typical scenario has been used to identify the propagation direction of the tsunami wave in front of the coasts of interest, at 50-m water depth, i.e. the offshore location at which the semi-analytical approach is applied. Figure 4 also shows that portions of the Apulian and Sicilian coasts experienced the most angled waves, i.e. respectively, inclined of ∼60° with respect to the direction orthogonal to the coast and almost parallel to the coast (Figure 4A and B).

3.2 Intermediate-scale modelling: α distribution along the southern Italian coasts

The parameter α has been computed along the Italian coasts by subdividing the interested coastlines into a number of domains of variable cross-shore and longshore sizes, generally in the order of 100–200 km (Figure 5a–b), to allow for a more detailed characterization of each coastal region. All grid sizes in both directions are set at 150 m. The bathymetries have been smoothed with a median filter to remove occasional spikes and ensure a smooth wave transformation.

The α distribution for the investigated coasts is given in Figure 5c–d. The values of α have been evaluated from the outcome of intermediate-scale simulations with SASHA: small and high values of α are indicative of low tsunami impact (small residual energy flux at 5 m depth) and high tsunami impact (high residual energy flux at 5 m depth), respectively.

The smallest values of α are observed in areas that are less exposed to the action of a tsunami at a realistic attack angle, due to their favourable geographical location. The coast north of the Apulia Region (Figure 5c) is characterized by small values of α

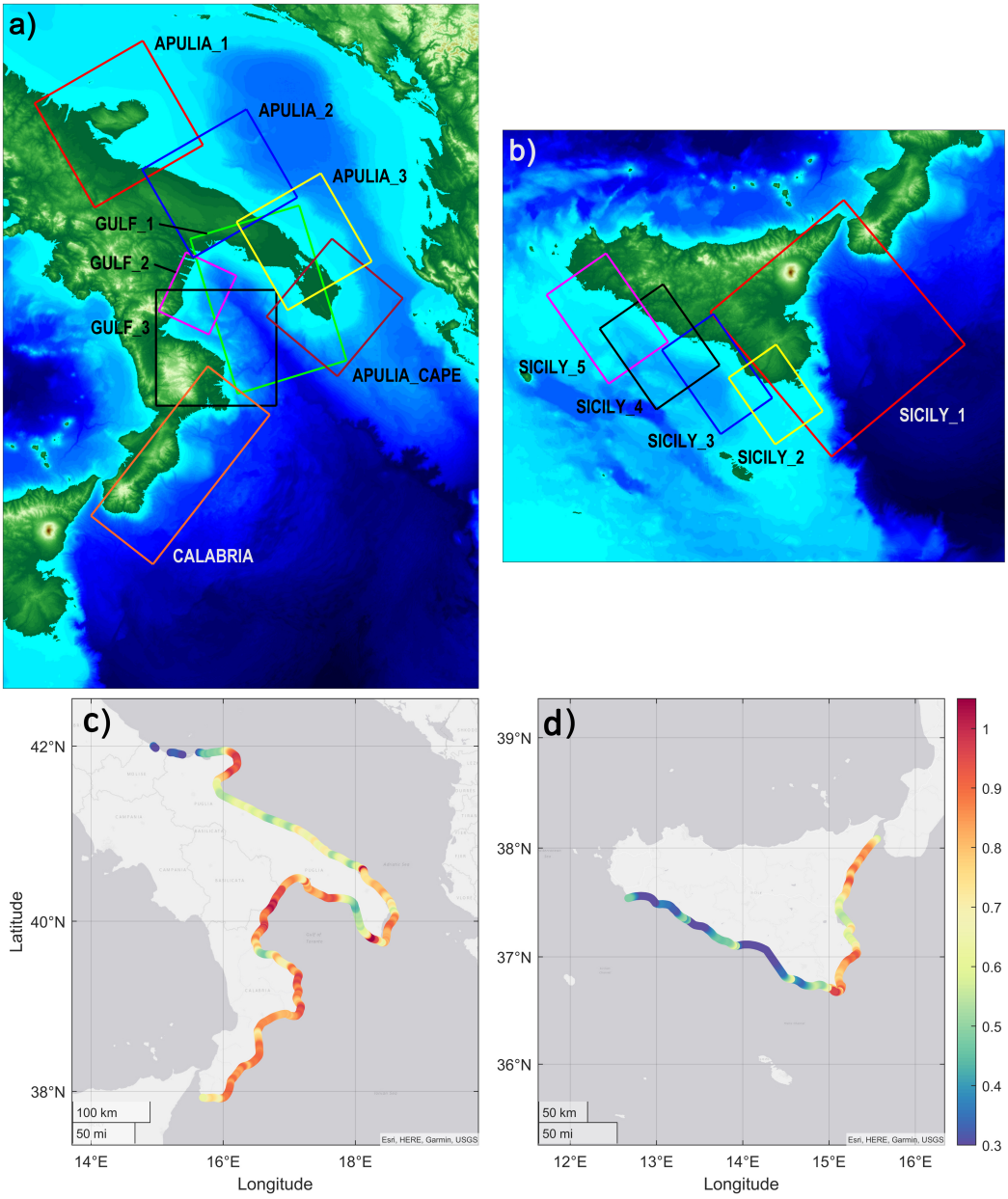

Figure 5. Domains used for the SASHA simulation campaign and distribution of the parameter α evaluated through the semi-analytical approach for **a, c)** peninsular Italy (Apulia, Basilicata, Calabria), and **b, d)** Sicily.

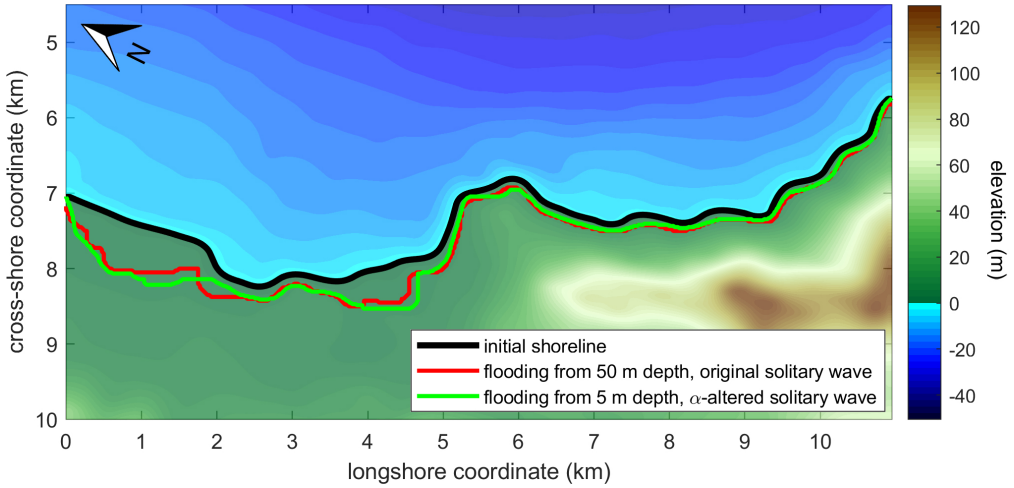

Figure 6. Area around the Esaro River estuary, used as numerical domain for the small-scale modelling, and comparison of shorelines simulated with the tested approaches: initial shoreline (black line), maximum inundation of a 2-m solitary wave at a 50-m depth (red line), maximum inundation of the α-scaled solitary wave (3.03 m wave height) imposed at 5-m depth (green line).

(< 0.4), as it is protected by the Gargano Promontory, which is in turn much more susceptible to tsunami energy ($\alpha > 1$). A similar behavior is observed in Sicily (Figure 5d), whose southern and western coasts ($\alpha < 0.4$) are more protected than the eastern coasts ($\alpha \approx 1$). The whole Calabria coast is highly impacted by the tsunami wave, with α oscillating around 1 almost everywhere, with the most exposed area being that of the Taranto Gulf. Less impacted is the Adriatic Apulia coast, with $\alpha \approx (0.5-0.6)$ on average, while the southernmost part of Apulia is highly exposed ($\alpha \approx 1$).

3.3 Small-scale modelling: nearshore propagation and flooding

As an illustrative example, α evaluated in the intermediate-scale modelling campaign and pictured in Figure 5c–d are exploited to model flooding levels in the coastal region surrounding the Esaro River estuary (Calabria). The chosen location is characterized by an urbanized setting with industrial, residential and recreational areas, and is thus representative of a typical Italian coastal environment.

Shallow-water, small-scale coastal modelling is performed using FUNWAVE-TVD on a computational domain with a maximum offshore depth of 5 m (i.e. the depth at which α is evaluated). Now, the definition of wave input for this simulation implements

the concept of α as a proxy of seabed-induced effects; that is, the wave form used as input for intermediate-scale modelling (50 m) is "scaled" through α to reduce it at 5-m depth. The "scaled" wave input is then applied as an initial condition of water surface displacement at a water depth 5 m and used to evaluate coastal flooding. The scaling is performed with the formulas given in Section 2.4. With the use of α, all bathymetry-related dynamics influencing the solitary wave height (shoaling, refraction, diffraction) are included when transporting wave data from intermediate to shallow waters. This application allows us to show that a good representation of tsunami-induced inundation can also be achieved with input data from simpler, linear tools and semi-analytical concepts.

In the example we assume that the tsunami height at $d_0 = 50$ m is $H_0 = 2$ m. Provided that the mean value of α along the considered coast is 0.853, the "scaled" input wave to be imposed at $d_1 = 5$ m depth would have a wave height $H_1 = 3.03$ m and a wavelength $L_1 = 573.57$ m.

We make a comparison of coastal flooding levels obtained with the two previously mentioned approaches: (i) intermediate-scale simulation on a 25×25 m grid with a 2-m solitary wave at offshore depth 50 m, and (ii) small-scale simulation on a 15×15 m grid with a 3.03-m "scaled" wave at offshore depth 5 m. Figure 6 shows maximum shoreline motions for both approaches. The two modelled shorelines are overall in good agreement, lending support to a fruitful use of α as a tool to move modelling efforts towards smaller scales once offshore tsunami data are known, by either observation or previous modelling. In this application, the small-scale simulation achieved a reduction of about 41% in computational time with respect to the intermediate-scale simulation.

4 Discussion and Conclusions

The method and application here proposed have shown that once the α parameter is defined and available in a specific coastal area, coastal inundation can be evaluated by running only a small-scale simulation over the coast of interest, while pre-defined information (e.g., wave direction and α) are known beforehand to speed up the whole forecasting process. The method allows for the down-scaling of computational effort towards small regional scales once information from a relatively coarser basin-scale simulation is available. This help complying with the need of fast (typically, within a few

minutes), yet reliable deterministic first estimates of tsunami impact (Selva et al., 2021) only in the region of interest.

The modelling chain has its starting point in the definition of a prototypical tsunami based on a real, catastrophic event. In this regard, the procedure proposed here is similar to a worst-case plausible scenario. The analysis of a limited number or even single scenarios may be put in tandem with previous probabilistic hazard assessments (like those described in Tonini et al. (2021) and Selva et al. (2021)) in the perspective of narrowing tsunami variability down to a range of most probable parameters.

The method is also valuable when precise forecasting of flooding is needed. In fact, underestimation of tsunami features may lead to fatal missed alarms, as occurred during the 2011 Tohoku tsunami event, when the tsunami height was initially underestimated, and so the inundated coastal area. This led to a number of casualties much larger than those that could have been suffered with a more accurate forecasting (Makinoshima et al., 2021).

It is worthwhile to notice that the semi-empirical implementation of the Green's law explicitly accounts for the effects of the bathymetry over the deformation of the wave front and, eventually, over tsunami impact. Bathymetry effects are inherently neglected in non-probabilistic procedures for tsunami-related alert states like decision matrices (Selva et al., 2021), and circumvented by end-to-end forecasting methods like neural networking (Makinoshima et al., 2021). On the other hand, probabilistic methods deal with the unknown effects of bathymetry only with varying uncertainty bounds on forecast results (Selva et al., 2021).

The methodology could be further improved by tackling other sources of uncertainty, like fault orientation and the subsequent main direction of propagation (Selva et al., 2021). With additional work on code optimization and automation, the procedure could also be applied to sources with general initial surface displacements, possibly evaluated as a function of earthquake parameters.

5 Acknowledgements

The study is funded by Circeo National Park and Gargano National Park within the National Biodiversity Strategy promoted by the Ministero dell'Ambiente e della Tutela del Territorio e del Mare (MATTM), Italy (GAB0024444). Support from the Office of

Naval Research Global (UK) MORSE Project (Research Grant Number N62909-17-1-2148), the MIUR PRIN 2017 Project "FUNdamentals of BREAKing wave-induced boundary dynamics – FUNBREAK" (Grant Number 20172B7MY9), and the Italian Civil Protection in the framework of the Italian Tsunami Directive is gratefully acknowledged.

6 Open Research

A dataset including input and output data for the presented simulations is available at the Zenodo repository referenced in Melito et al. (2022). Version 3.6 of the software Funwave has been used for hydrodynamic modelling; the model is in the public domain and can be downloaded at the following page: `https://github.com/fengyanshi/FUNWAVE-TVD/releases/tag/Version_3.6`. Bathymetries are freely available at the GEBCO platform: `https://www.gebco.net`.

References

Ambraseys, N., & Synolakis, C. (2010). Tsunami catalogs for the Eastern Mediterranean, revisited. *Journal of Earthquake Engineering*, *14*(3), 309–330.

Anfuso, G., Postacchini, M., Di Luccio, D., & Benassai, G. (2021). Coastal sensitivity/vulnerability characterization and adaptation strategies: a review. *Journal of Marine Science and Engineering*, *9*(1), 72.

Bonaldo, D., Antonioli, F., Archetti, R., Bezzi, A., Correggiari, A., Davolio, S., ... others (2019). Integrating multidisciplinary instruments for assessing coastal vulnerability to erosion and sea level rise: Lessons and challenges from the Adriatic Sea, Italy. *Journal of Coastal Conservation*, *23*(1), 19–37.

Chaib, W., Guerfi, M., & Hemdane, Y. (2020). Evaluation of coastal vulnerability and exposure to erosion and submersion risks in Bou Ismail Bay (Algeria) using the coastal risk index (CRI). *Arabian Journal of Geosciences*, *13*(11), 1–18.

Da Lio, C., & Tosi, L. (2019). Vulnerability to relative sea-level rise in the Po river delta (Italy). *Estuarine, Coastal and Shelf Science*, *228*, 106379.

Dean, R. G., & Dalrymple, R. A. (1991). *Water Wave Mechanics for Engineers and Scientists* (Vol. 2). World Scientific. doi: 10.1142/1232

Federico, I., Pinardi, N., Coppini, G., Oddo, P., Lecci, R., & Mossa, M. (2017). Coastal ocean forecasting with an unstructured grid model in the southern

Adriatic and northern Ionian seas. *Natural Hazards and Earth System Sciences*, *17*(1), 45–59.

Fujii, Y., Satake, K., Sakai, S., Shinohara, M., & Kanazawa, T. (2011). Tsunami source of the 2011 off the Pacific coast of Tohoku Earthquake. *Earth Planets Space*, *63*(7), 815–820. doi: 10.5047/eps.2011.06.010

Gaeta, M. G., Bonaldo, D., Samaras, A. G., Carniel, S., & Archetti, R. (2018). Coupled wave-2d hydrodynamics modeling at the Reno river mouth (Italy) under climate change scenarios. *Water*, *10*(10), 1380.

Hzami, A., Heggy, E., Amrouni, O., Mahé, G., Maanan, M., & Abdeljaouad, S. (2021). Alarming coastal vulnerability of the deltaic and sandy beaches of North Africa. *Scientific reports*, *11*(1), 1–15.

Lalli, F., Berti, D., Miozzi, M., Miscione, F., Porfidia, B., Serva, L., ... others (2001). Analysis of breakwater-induced environmental effects at Pescara (Adriatic Sea, Italy) channel-harbor. In *The eleventh international offshore and polar engineering conference.*

Lalli, F., Bruschi, A., Lama, R., Liberti, L., Mandrone, S., & Pesarino, V. (2010). Coanda effect in coastal flows. *Coastal Eng.*, *57*(3), 278–289.

Lalli, F., Postacchini, M., & Brocchini, M. (2019). Long waves approaching the coast: Green's law generalization. *J. Ocean Eng. Marine Energy*, *5*(4), 385–402. doi: 10.1007/s40722-019-00152-9

Lay, T., Kanamori, H., Ammon, C. J., Nettles, M., Ward, S. N., Aster, R. C., ... others (2005). The great Sumatra-Andaman earthquake of 26 December 2004. *Science*, *308*(5725), 1127–1133. doi: 10.1126/science.1112250

Madsen, P. A., Fuhrman, D. R., & Schäffer, H. A. (2008). On the solitary wave paradigm for tsunamis. *Journal of Geophysical Research: Oceans*, *113*(C12).

Makinoshima, F., Oishi, Y., Yamazaki, T., Furumura, T., & Imamura, F. (2021). Early forecasting of tsunami inundation from tsunami and geodetic observation data with convolutional neural networks. *Nature Communications*, *12*(1), 1–10.

Maramai, A., Brizuela, B., & Graziani, L. (2014). The Euro-Mediterranean tsunami catalogue. *Ann. Geophys.-Italy*, *57*(4). doi: 10.4401/ag-6437

Maramai, A., Graziani, L., & Brizuela, B. (2021). Italian Tsunami Effects Database (ITED): The first database of tsunami effects observed along the Italian coasts.

Front. Earth Sci., *9*, 137. doi: 10.3389/feart.2021.596044

Mattei, G., Rizzo, A., Anfuso, G., Aucelli, P., & Gracia, F. (2019). A tool for evaluating the archaeological heritage vulnerability to coastal processes: The case study of Naples Gulf (southern Italy). *Ocean & Coastal Management*, *179*, 104876.

Melito, L., Lalli, F., Postacchini, M., & Brocchini, M. (2022). *Simulation data for a semi-empirical approach for tsunami inundation in South Italy* [dataset]. Zenodo. doi: 10.5281/zenodo.6249936

Mori, N., Takahashi, T., Yasuda, T., & Yanagisawa, H. (2011). Survey of 2011 tohoku earthquake tsunami inundation and run-up. *Geophysical Research Letters*, *38*(7).

Postacchini, M., Lalli, F., Memmola, F., Bruschi, A., Bellafiore, D., Lisi, I., ... Brocchini, M. (2019). A model chain approach for coastal inundation: Application to the bay of Alghero. *Estuarine, Coastal and Shelf Science*, *219*, 56–70.

Postacchini, M., & Ludeno, G. (2019). Combining numerical simulations and normalized scalar product strategy: A new tool for predicting beach inundation. *Journal of Marine Science and Engineering*, *7*(9), 325.

Satake, K. (1988). Effects of bathymetry on tsunami propagation: Application of ray tracing to tsunamis. *Pure and Applied Geophysics*, *126*(1), 27–36.

Selva, J., Lorito, S., Volpe, M., Romano, F., Tonini, R., Perfetti, P., ... others (2021). Probabilistic tsunami forecasting for early warning. *Nature Communications*, *12*(1), 1–14.

Shi, F., Kirby, J. T., Harris, J. C., Geiman, J. D., & Grilli, S. T. (2012). A high-order adaptive time-stepping TVD solver for Boussinesq modeling of breaking waves and coastal inundation. *Ocean Modelling*, *43*, 36–51.

Stiros, S. C. (2001). The AD 365 Crete earthquake and possible seismic clustering during the fourth to sixth centuries AD in the Eastern Mediterranean: a review of historical and archaeological data. *Journal of Structural Geology*, *23*(2-3), 545–562.

Tonini, R., Di Manna, P., Lorito, S., Selva, J., Volpe, M., Romano, F., ... Vittori, E. (2021). Testing Tsunami Inundation Maps for Evacuation Planning in Italy. *Frontiers in Earth Science*, *9*. doi: 10.3389/feart.2021.628061

Weatherall, P., Marks, K. M., Jakobsson, M., Schmitt, T., Tani, S., Arndt, J. E., ... Wigley, R. (2015). A new digital bathymetric model of the world's oceans. *Earth and Space Science*, *2*(8), 331–345.